# Laser-guided, intersecting discharge channels for the final beam transport in heavy-ion fusion

C. Niemann,[a] S. Neff, A. Tauschwitz, D. Penache, R. Birkner, C. Constantin,[a]
R. Knobloch, R. Presura,[b] F. B. Rosmej, and D. H. H. Hoffmann
*Technische Universitaet Darmstadt, Schlossgartenstrasse 9, 64289 Darmstadt, Germany*

S. S. Yu
*Lawrence Berkeley National Laboratory, 1 Cyclotron Road, Berkeley, California 94720*

(Received 15 November 2002; accepted 28 February 2003)

Ion-beam transport in space charge neutralizing discharge channels has been proposed for the final focus and chamber transport in a heavy-ion fusion reactor. A driver scenario with two-sided target illumination requires a system of two intersecting discharges to transport beams of the same charge from opposite sides towards the fusion target. In this article we report on experiments on the creation of free-standing, intersecting high-current discharge channels. The discharges are initiated in ammonia gas ($NH_3$) in a metallic chamber by two perpendicular $CO_2$-laser beams, which resonantly heat and subsequently rarefy the gas along the laser paths before the breakdown. These low density channels guide the discharges along the predefined paths and also around the 90° angles without any mechanical guiding structures. In this way stable X-, T-, and L-shaped discharges with currents in excess of 40 kA, at pressures of a few mbar were created with a total length of 110 cm. An 11.4 A MeV $^{58}Ni^{+12}$ beam from the UNILAC (Universal Linear Accelerator) linear accelerator was used to probe the line-integrated ion-optical properties of the central channel in a T-shaped discharge. © *2003 American Institute of Physics.* [DOI: 10.1063/1.1569395]

## I. INTRODUCTION

Plasma-channel based final beam focus and transport is an interesting alternative to other transport modes in the target chamber of a heavy-ion beam fusion reactor.[1–4] A plasma-channel based reactor with two sided target illumination requires two discharges and one or more current-return paths in order to provide a focusing magnetic field for two beams of the same charge, propagating from opposite sides towards the fusion target.[5] The feasibility of producing multiple intersecting channels has already been demonstrated in the seventies by laser-induced, aerosol-initiated air-breakdown guided V-shaped discharges.[6] However, due to the high required gas pressure and the poor stability of the channels, this method is not suited for a reactor application. Experiments on multiple discharges were also performed with exploding wires.[7] In those experiments a 30 cm long center channel and two current return paths with a length of 10 cm were initiated, at discharge currents of up to 40 kA. In ion-beam transport experiments a 14 kA, 1.1 MeV proton beam from the Reiden IV pulsed power machine was transported through the center channel with high efficiency.[8] Experiments in Berkeley on ultraviolet (UV)-laser initiated discharge channels produced two converging discharges from opposite sides towards a brass ball target in the center of the discharge chamber, connected by one or two metallic rods for the current return.[9–11] These experiments produced unstable channels with a single sided brass rod return path perpendicular to the laser initiated channels but demonstrated a very stable interaction with the target in a symmetric arrangement with a two-sided return path. However, for inertial-fusion energy, mechanical structures for the current return can not be used inside the reactor chamber, since they would be destroyed in every pellet explosion.

In an experiment at the Gesellschaft für Schwerionenforschung (GSI) described in the following, intersecting, free-standing discharges were initiated by two perpendicular laser beams without any other guiding structures at pressures of only a few mbar. Two channels with a length of 29 and 21 cm, respectively, converging linearly from opposite sides towards the intersection point (IP) together with two 30 cm long current-return channels, perpendicular to the other two discharges, were produced. The discharge channels are guided by two perpendicular $CO_2$ laser beams, which are resonantly absorbed in low pressure ammonia gas. The two laser beams meet exactly in the IP in the center of the discharge chamber. As the heated gas expands, a gas-rarefaction channel of the shape of a cross is formed along the laser beams, with preferred breakdown conditions for the subsequent high-current discharge. Therefore the discharge channels are guided along the laser paths and around the corners. With this technique it was possible to produce L-, T-, and X-shaped, free-standing discharges with a total length of 110 cm (see Sec. III). Beam transport experiments with an 11.4 AMeV $^{58}Ni^{+12}$ beam from the GSI linear accelerator, which was used to analyze the ion-optical properties of the discharge, will be presented in Sec. IV.

## II. EXPERIMENTAL SETUP

The discharges are created in a cylindrical stainless-steel chamber of 50 cm length and 60 cm diameter, filled with

[a]Present address: Lawrence Livermore National Laboratory, 7000 East Avenue, Livermore, CA 94550; electronic mail: niemann1@llnl.gov
[b]Present address: University of Nevada, Reno, NV 89557.

 

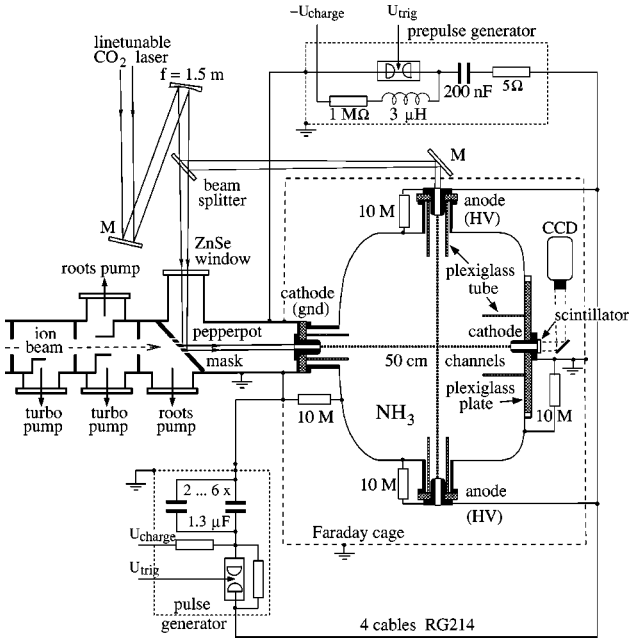


FIG. 1. Experimental setup for the intersecting channels.

ammonia gas ($NH_3$) at pressures below 10 mbar. Four stainless-steel electrodes are mounted on opposite sides, insulated from the chamber by plexiglass flanges. Two cathodes are located at the symmetry axis of the chamber while two anodes are oriented perpendicularly. All four electrodes are arranged in the same plane, indicating the shape of a cross (Fig. 1). The discharges are guided by two $CO_2$-laser beams in the chamber. Resonant absorption of the laser with its wavelength tuned to the vibrations of the ammonia molecules leads to a strong heating and subsequent rarefaction of the gas. The laser-gas interaction and channel-initiation mechanism were studied previously for straight discharges at GSI[12] and elsewhere.[13–15] An $f=1.5$ m concave mirror focuses the laser before it is split into two beams of equal intensity by a 50/50 beam splitter. Both beams enter the discharge chamber through ZnSe–vacuum windows and 15 mm bore holes in the upper anode and the left cathode. The two laser beams meet in the center of the chamber, which is also the position of the beam waists, and form the shape of a cross. The footprint of the rectangular beam profiles varies only slightly from 0.9 $cm^2$ in the focus to 1.1 $cm^2$ near the electrodes. In each beam the maximum energy density was around 1 $J/cm^2$. Four plexiglass tubes extend 10 cm from all four electrodes into the chamber to prevent breakdown directly to the metallic wall. A few microseconds after the laser pulse a capacitor bank of 1.3–7.8 $\mu$F, charged to 20 kV is connected to the electrodes by a spark-gap switch, and the discharge channels are formed along the laser paths. A low energy predischarge can optionally be applied before the high-current discharge from a second pulse generator with a 200 nF capacitor, charged to a few kV. This predischarge was designed to stabilize or shape the subsequent high-current discharge. The main-pulse generator is connected by two RG214 high-voltage cables of 3 m length to each of the anodes, which are at the same potential. Two 10 cm wide and 70 cm long copper bands, that connect the two cathodes. The ground of the high-voltage cables is connected symmetrically to these copper bands in the middle between both cathodes. Both pulse generators as well as the discharge chamber are enclosed in Faraday cages with only small entrance ports for the laser beams and the diagnostics to shield the electromagnetic noise.

For the beam-transport experiments the discharge chamber was integrated into the Z4 beamline of the GSI UNILAC (Universal Linear Accelerator) linear accelerator. Since the maximum available particle energy is 13 A MeV and the stopping power in matter is rather high, an entrance window from the accelerator to the discharge chamber can not be used. Therefore a 2 m long differential pumping section consisting of several roots- and turbo-pumps reduces the pressure gradually from initially a few mbar inside the chamber down to the $10^{-6}$ mbar environment of the accelerator-beam pipe. A molybdenum pepperpot mask, which is also used as a final bending mirror for one of the two laser beams, prepares nine circular ion beamlets from the whole UNILAC beam oriented in the shape of a cross. A fast plastic scintillator, mounted in a 15 mm diam hole in the back side cathode, in combination with a fast shutter camera is used to analyze the temporal shift of the individual beamlets and thus the line integrated ion optical properties of the channels, as the magnetic field of the discharge evolves (see Sec. IV).

## III. CREATION OF INTERSECTING DISCHARGES

In a low-current discharge from the prepulse generator (4.9 J, 1 kA), triggered a few microseconds after the laser pulse at a gas pressure of 5 mbar, the following discharge behavior is observed: instead of the two required intersecting discharges, only one L-shaped discharge with two straight channel sections and a bending radius not bigger than 10 mm at the IP is created. The channel does not take a shortcut through the unheated gas but follows at all times the laser beam and is therefore bent around the corner by 90°. Figure 2 shows two representative fast shutter camera images at different times, shortly after the breakdown, and around the current maximum. Dotted lines indicate the initial footprints of the two intersecting laser beams. Due to the narrow vacuum window only a 5 cm wide central section of the channels can be observed. Previous experiments on $CO_2$ laser initiated discharges in $NH_3$ have measured a reduction of the gas density of up to 70% for a laser energy density of around 2 $J/cm^2$ in 15 mbar.[12] With a $pd$ product of around $2\times10^2$ Torr cm the breakdown behavior is characterized by the linear right-hand side branch of the room temperature Paschen curve. The condition for the discharge to follow the laser path around the right angle instead of the shortest way through the unheated gas is a smaller $pd$ along the longer path due to a smaller local $p$. It follows easily from geometrical considerations that $pd$ along the laser becomes comparable or smaller than $pd$ along the diagonal, if the density along the laser is reduced by a factor of $1/\sqrt{2}\approx0.71$, which is readily fulfilled by the laser gas heating.

The formation of the L discharge can be explained as follows: the laser energy is not absorbed homogeneously in-

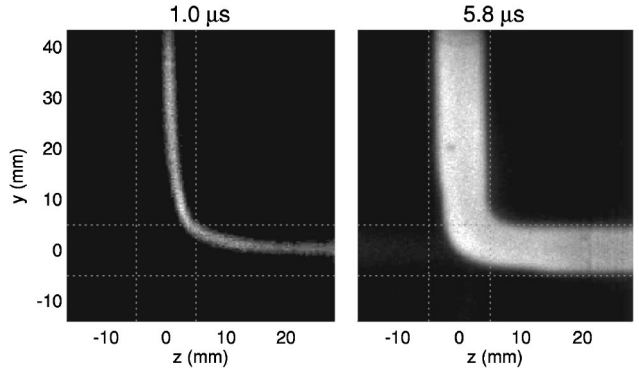


FIG. 2. Fast-shutter camera images of a low-current discharge in 5 mbar ammonia for two different times after the breakdown. Due to the size of the vacuum windows only the 5 cm wide central section of the channels can be observed. The dotted lines indicate the footprints of the laser beams.

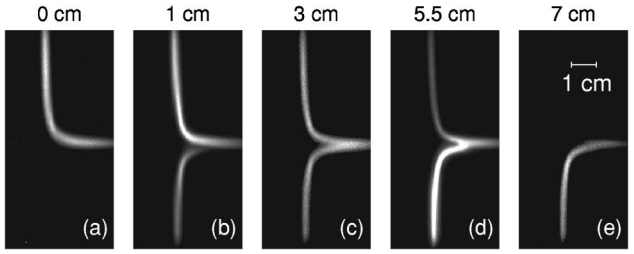


FIG. 3. Current balancing by an impedance matching: different discharges produced with a metal rod of different length, extending the lower anode towards the intersection point. The pictures were all recorded 2 $\mu$s after the voltage breakdown.

side the chamber. Along the laser path, the absorption $\partial I(z)/\partial z$ varies proportional to $\sigma \cdot I(z)$, where $I(z)$ is the laser energy at the position $z$ and $\sigma$ the absorption-cross section. Apart from saturation effects ($\sigma \equiv \sigma(I)$), which were observed in previous experiments,[12,13] this leads to an exponential decrease of deposited energy along the laser path. Consequently, the gas near the left cathode and the upper anode is heated stronger than the gas near the right cathode and the bottom anode, which leads to a better gas rarefaction and preferred conditions for the discharge. Besides, the discharge chamber is not symmetric along the ion-beam axis (left–right). The distance from the left anode to the IP of the crossed channels (29 cm) is bigger than the distance from the IP to the right anode (21 cm). As a consequence of this impedance imbalance the entire discharge current flows only through the upper and right channel sections and an L channel is formed. The deficient gas rarefaction near the bottom anode can be compensated by a shorter distance between this anode and the IP. This current or $pd$ balancing was realized by a 1 cm diam stainless steel rod of adjustable length, extending the bottom anode towards the IP, to match the impedances of the upper and lower channel sections. The effect of the rod is illustrated in Fig. 3. Without the extension rod the current flows entirely through the upper channel section (a). A rod with only 1 cm length already draws a visible fraction of the current towards the bottom anode (b). A 3 cm long rod yields in this conditions an almost perfect current balance between the upper and the lower channel section (c). At an even shorter distance between the IP and the lower anode, the breakdown occurs only towards the bottom anode (e). The balance depends very sensitively on the laser absorption and thus on the gas pressure and the laser wavelength.[12] At a higher gas pressure, the temperature difference between the laser heated gas near the entrance and the exit anode is even more emphasized. A balanced system, creating a T channel at a certain pressure will create an L-shaped discharge upwards at higher pressures and an L-discharge downwards at lower pressures. A pressure difference of less than 1/2 mbar was in this experiment sufficient to compensate a rod length of 1 cm, which is in agreement with the Paschen law. After some microseconds a T-shaped discharge transforms into an L discharge when the channel section with the larger initial discharge current builds up even better conditions for the discharge (higher conductivity, lower impedance), compared to the other channel section. In the experiments the duration of the T-channel phase, where two current return paths can exist simultaneously, could be increased to almost the duration of the discharge by a proper $pd$ balancing. X-shaped low-current discharges or L discharges from the left cathode towards the top or bottom anode were also created at slightly higher pressures of up to 10 mbar. However, the asymmetric chamber geometry and laser absorption did not allow a reproducible initiation of X-shaped discharges and lead to the transformation of X into T discharges a few microseconds after the breakdown. In channel–target interaction experiments (see also Sec. V), a laser-beam stop near the IP was used to prevent gas heating and to artificially increase the $pd$ product only in the right horizontal channel section. In this condition L- or T-shaped discharges were produced only towards the left cathode. This demonstrates that X-shaped discharges should be easily produced in a symmetric chamber, as it will be used for a fusion reactor. For UV-laser initiated[10] or ion-beam initiated discharges,[16] where the initial conditions are considerably more symmetric along the laser paths than in our case, the current balancing of intersecting discharges should also be much easier. The experiments performed in Berkeley, with metal rods replacing the second perpendicular discharge, produced two converging channels simultaneously each time.[10,11] However, a small current imbalance due to an impedance imbalance was also observed there.

Also the high-current discharge (40 kA) follows the laser footprints to form a T-shaped plasma channel. In the experiments it was not possible to produce L-shaped high-current channels. Even with an extending metal rod of several cm length at one of the electrodes and / or a preceding L-shaped low-current discharge, the subsequent high-current discharge forms a T channel. The formation of multiple channels is therefore easier at higher discharge currents. A series of fast shutter photographs of the high-current discharge at different times after the breakdown is shown in Fig. 4. The temporal evolution shows two separate L channels near the IP at early times, with a bending radius of a few mm. After 2 $\mu$s the two horizontal channels, which are separated by a few mm close to the IP, merge to one. The discharges are surprisingly stable up to late times after the current maximum. After a few microseconds, a displacement of the two vertical channel sec-

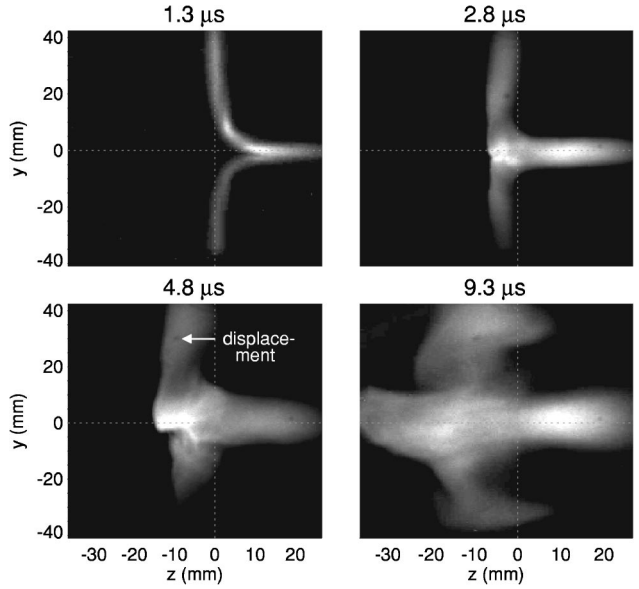


FIG. 4. A series of pictures of a T-shaped high-current discharge in 5 mbar. A maximum discharge current of 40 kA is reached after 4 $\mu$s. The dotted lines indicate the position of the two laser beams.

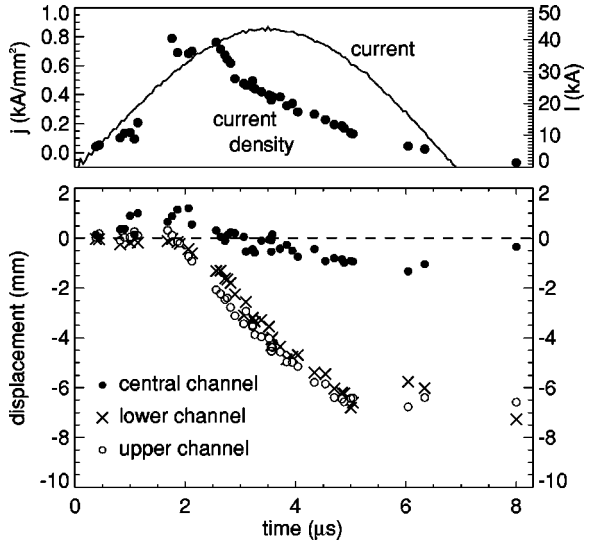


FIG. 5. Magnetic forces at the intersection point cause a displacement of the upper and lower channel section towards the left side. The central channel is only slightly displaced downwards, since the azimuthal magnetic field of the upper and lower current-return channel cancel each other almost entirely.

tions of a few mm towards the left side can be observed. Due to the 90° angles, the two current-return channels experience the azimuthal magnetic field of the center channel. The higher magnetic pressure inside the bending section results in a net force towards the left side. This force decreases with the distance y from the IP. The center channel is not displaced since the opposite currents from the two return channels just compensate. Figure 5 compares the displacement of the three channel sections in a T-shaped high-current discharge as a function of time. The current density $j = I/(\pi \cdot r^2)$ was calculated from the total discharge current $I$ and the channel diameter (full with half maximum), which was determined from the fast-shutter photographs of the plasma-self emission. Around 2 $\mu$s after the breakdown the discharge pinches and the smallest channel diameter and thus the highest current density is reached. While the current density is large enough (1 $\mu$s until 6 $\mu$s) the upper and lower channel sections are displaced. As the discharge current decreases and the channel expands strongly after the current maximum, the displacement saturates at a value of 6 to 8 mm. In an X-shaped discharge with proper current balancing the magnetic fields of all four channel sections cancel and none of the channels is displaced.

## IV. ION-BEAM TRANSPORT EXPERIMENTS

An 11.4 A MeV $^{58}Ni^{+12}$ beam from the 100 m long UNILAC linear accelerator at GSI was used to probe the ion-optical properties of the discharge and thus the azimuthal magnetic field and the current-density distribution inside the plasma. For this purpose nine circular 1 mm diam beamlets were selected in a cross shaped configuration from the 15 mm diameter Gaussian ion beam by a molybdenum-pepperpot mask. The holes in the mask were distributed equally along the $x$ and $y$ axis with a distance of 1 mm between the holes. The central hole was missing and one additional hole was located at an asymmetric position at 45°. The azimuthal magnetic field of the discharge bends these beamlets towards the discharge axis, depending on their radial position. Positively charged ions, which enter the channel along the direction of the discharge-current flow (from the anode to the cathode), are bent towards the discharge axis while ions propagating in opposite direction are bent outwards and the beam is defocused. An X-shaped discharge can not be diagnosed by the ion beam since the ions would be transported only up to the IP before the beam is defocused. A T-shaped discharge was used instead to investigate the effect of the IP on the overall ion-optical properties of the discharge. The beam initially drifts through the first half of the discharge chamber without the influence of a magnetic field and is then transported through the right horizontal plasma channel, which provides a focusing azimuthal magnetic field. A fast plastic scintillator (Bicron BC-400) inside the hollow cathode was used to visualize the ion distribution behind the chamber. A total ion-beam current of around 50 $\mu$A before the pepperpot mask allowed an exposure time as low as 30 ns with an image intensified camera, which is fast enough compared to the dynamics of the discharge. The high ion-beam current causes a rapid aging of the scintillator material, which must be replaced frequently. Scintillator light emission due to the laser beam and the discharge itself is prevented by a thin Al foil in front of the scintillator with a negligible energy loss of the ion beam. Both, the ion and the laser beam as well as the center of the pepperpot cross are aligned to the symmetry axis of the discharge chamber. However, due to the large laser beam size ($\sim$10 mm) an uncertainty in the position of the discharge axis of a few mm is typical. If the discharge axis is not exactly aligned to the center of the pepperpot cross, the beamlets are deflected towards a point, which indicates the actual discharge axis as soon as a magnetic field is present. Figure 6 shows the

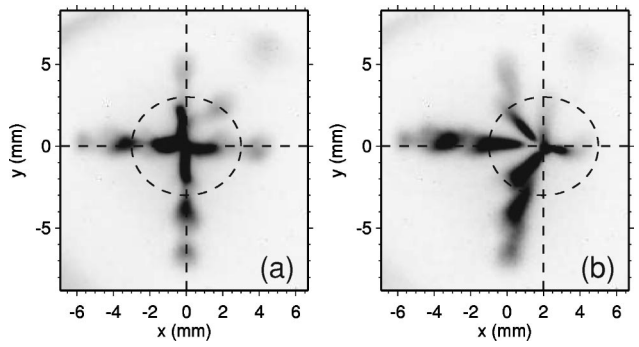


FIG. 6. Fast-shutter photographs of the scintillator-light emission caused by the heavy-ion beam behind the discharge channel for a discharge aligned exactly to the ion-beam axis (a) and the discharges displaced by 2 mm in the $x$ direction (b). The exposure time was 1 $\mu$s to image the trend of the beamlet motion towards the point, that indicates the discharge axis (dashed lines).

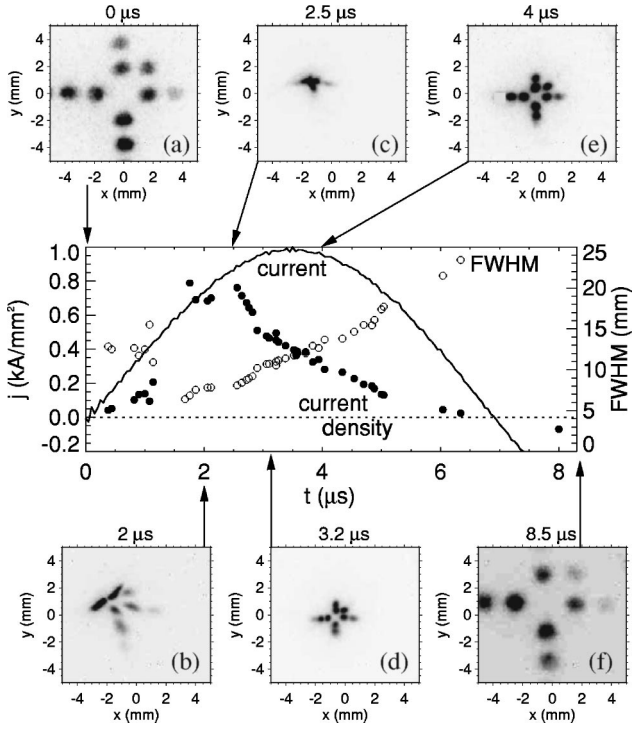


FIG. 7. Photographs of the scintillator light emission for different times during the discharge as well as the discharge current. The exposure time was 30 ns each time. A focus can be observed at around 2.7 $\mu$s.

scintillator-light emission for two discharges with different axis relative to the pepperpot cross. During the exposure time of 1 $\mu$s the magnetic field in the plasma changes and the beamlets are streaked towards the discharge axis. While Fig. 6(a) represents a discharge with a perfect alignment in Fig. 6(b) the laser beam and thus the channel axis were displaced by 2 mm in the $x$ direction. The trend of the beamlets clearly points towards the new discharge axis, which is marked by the dotted lines. This behavior demonstrates, how sensitively the discharge follows the laser beam. In the experiments this method was used to optimize the alignment of the laser and the ion beam.

A series of fast-shutter photographs of the scintillator-light emission with an exposure time of 30 ns is shown in Fig. 7, together with the discharge-current evolution. The picture (a) shows an image of the original pepperpot cross without the discharge. At 2 $\mu$s after the breakdown the beamlets are focused slightly towards the discharge axis (b). The shape of the cross is strongly distorted, which indicates an inhomogeneous current-density distribution. At this time, when the discharge pinches to its smallest diameter, the channel is smaller than the size of the pepperpot cross, leaving the outer most beamlets in a region where the magnetic field decreases nonlinearly with the distance from the discharge axis. As the current density rises the pepperpot cross is focused to smaller sizes. The smallest focus is reached at around 2.5 $\mu$s (c). The focusing strength then decreases in time as the discharge current drops and the channel expands. At very late times (f), the reversed current flow leads to a defocusing of the beamlets, and the pepperpot image is magnified. Apart from the pinchtime ($\sim 2$ $\mu$s), the scintillator shows always an almost undistorted, scaled image of the pepperpot mask. This is an indication that—apart from the pinchtime—the discharge behaves like an ideal ion-optical element with a homogeneous current-density distribution and consequently a linear magnetic field inside the plasma.

Simulations with a simple Monte Carlo code were compared to the experimental scintillator images. The trajectories of an ion, propagating through the plasma channel, can easily be calculated from the Lorentz-force equation $\ddot{\mathbf{r}} = e \cdot C/(m_p \cdot A)\mathbf{v} \times \mathbf{B}$, where $m_p$ is the proton mass, $e$ the elementary charge, $A$ the number of nucleons, and $C$ the charge state of the ion. The charge state was estimated by the empirical Betz formula,[17] which gives the center of mass of the equilibrium charge state distribution after stripping of the ions in the gas of the differential pumping system. Inside the plasma channel, the charge state was assumed to remain constant. The Betz formula yields a charge state of 26 for the used 11.4 A MeV $^{58}_{28}Ni^{12+}$ beam. The transverse position of each beamlet is traced through the plasma channel, by numerically solving the equation of motion, and the expected scintillator image behind the discharge channel is constructed. A comparison between the measured and the simulated focusing strength of the discharge is given in Fig. 8(a). The graph shows the temporal evolution of the normalized size of the pepperpot cross, measured behind the channel. At the pinch time of the discharge at around 2 $\mu$s, the maximum current density distribution reduces the size of the pepperpot image by more than 80%. The results from the simulation, assuming a homogeneous current density distribution, show an excellent agreement with the measurements. The current density [Fig. 8(c)] was calculated from the total discharge current and the channel diameter as measured from the fast-shutter photographs of the plasma-self emission. This shows, that the entire discharge current flows through the plasma channel and not partially around the insulators in parasitic discharges. Figure 8(b) gives an overview of the distribution of the individual beamlets behind the channel. The inhomogeneity factors $f_x = (2 \cdot x - d)/d$ and $f_y = (2 \cdot y - d)/d$ are a measure of the deviation from a homogeneous current density distri-

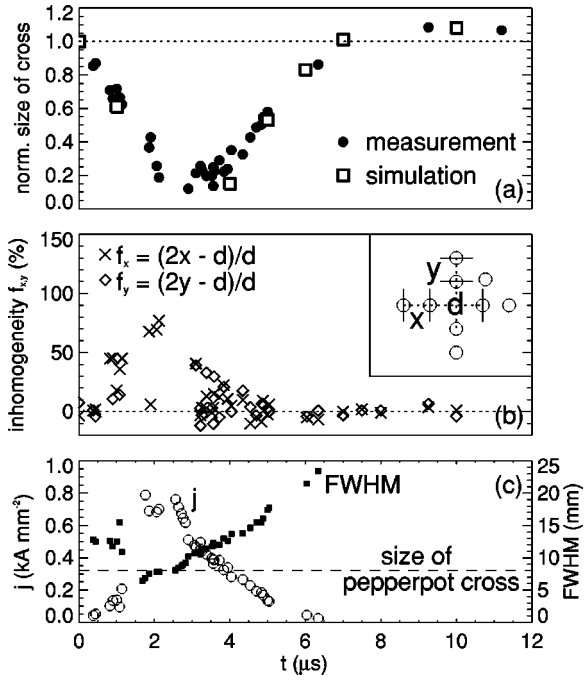


FIG. 8. Temporal evolution of the focusing strength of the discharge (a) and the deviation from a homogeneous current density distribution (b). The simulated points were obtained from ion-beam trajectory calculations with a homogeneous current density distribution. The inhomogeneity factor $f_{x,y}$ (b) is a measure of the deviation of the current density from a homogeneous distribution. In a perfect homogeneous current density channel $f$ would be exactly 0.

bution in the horizontal and vertical direction. A discharge with a perfect homogeneous current distribution and thus a linear magnetic field acts like an ideal ion-optical element. In this case the relative spacing between individual beamlets does not change with the magnetic field ($f_{x,y}=0$), while only the size of the pepperpot image is scaled. The factors $f_x$ and $f_y$ compare the relative spacings of the outer beamlets ($x$ or $y$) and the inner beamlets (d). As Fig. 8(b) shows, $f$ deviates from 0 by more than 50% during the pinch time of the discharge. This is partially due to the fact, that the channel diameter at this time is smaller than the pepperpot cross [Fig. 8(c)], leaving the outer beamlets in a region with a nonlinearly decreasing magnetic field. This is also in agreement with the fact that $f_{x,y}>0$, since the inner beamlets are focused stronger in this case. Already 3 $\mu$s after the breakdown and especially at the time of the current maximum (4 $\mu$s) or later, $f_{x,y}$ are close to 0 and thus the magnetic field inside the plasma is linear. These experiments demonstrate that a heavy ion beam can be transported through an intersecting discharge with high efficiency. The current density distribution is at most times such of an ideal ion-optical lens. The beam current distribution that enters the discharge channel is therefore reproduced behind the channel.

## V. CHANNEL–TARGET INTERACTION

The fusion targets will be injected into the reactor chamber with a repetition rate of a few Hz. The target injection velocity is small compared to the dynamical timescale of the plasma channel. Therefore the target will be in position before and during the discharges are initiated. Since the target will be in direct contact with the discharge plasma in the IP, the channel–target interaction has to fulfill two conditions: the discharge or the laser beams must not heat the pellet before the arrival of the ion beam pulse, and the pellet must not disturb the stability of the plasma channels. A simple target design to overcome those problems was proposed in Berkeley.[18] The actual indirect drive target is embedded in a conducting mesh with four thin metallic wires of a few cm length pointing towards the directions of the four channel sections. The wires serve as ''anchors'' for the discharges to intersect exactly at the target position. Due to the conducting mesh, the current is carried around the target and the fusion pellet is not heated by the discharge before the arrival of the ion-beam pulse. Preliminary experiments on the channel interaction with simple targets in the IP have been performed at GSI. The metal targets were mounted on a plastic rod, connected to the bottom anode, which allowed only interaction experiments with the three remaining channel sections. One of the targets used was a thin circular 1 cm diam copper sheet, with a circular 5 mm diam hole in the center, and three pins pointing towards the two cathodes and the upper anode. The experiments showed, that multiple channels (T channels) were more easily created with the target than without. An L-shaped discharge without the target turned in all cases into a T discharge as soon as the target was used, independent of the pressure. The discharges were completely separated by the target and the current in the IP was entirely carried inside the metal sheet as envisioned in the Berkeley target proposal. However, the electromagnetic field enhancing needles did not influence the breakdown behavior near the target. The breakdown path of the discharge was solely defined by the laser beam, independent of the position of the needles.

## VI. CONCLUSION

We demonstrated the feasibility to produce free-standing, intersecting $z$ discharges by $CO_2$–laser initiation in ammonia gas. This method allowed to create L-, T-, and X-shaped discharges with currents in excess of 40 kA at pressures below 10 mbar. A current imbalance, due to an impedance imbalance was observed, and can be explained by the inhomogeneous laser-energy absorption along the laser path and the asymmetric chamber geometry. It was demonstrated, that this current imbalance can be compensated by a proper impedance matching. T-shaped high-current discharges with a current of more than 40 kA were stable for times longer than the current rise time.

It was shown that two symmetric current-return paths compensate the net magnetic field acting on the central discharge channel, which is stabilized in this way. The magnetic forces near the intersection point in an asymmetric arrangement on the other hand, lead to a displacement of the discharges by several mm.

Ion-beam transport experiments with an 11.4 A MeV $^{58}Ni^{12+}$ beam showed that the magnetic field of the 21 cm long central section of a 40 kA T-shaped discharge is sufficient to transport the ion beam over almost one half of a

betatron oscillation. Measurements of the ion-optical properties of the discharge show an excellent agreement to simulations with a simple Monte Carlo code. Apart from the pinch time of the discharge, the current-density distribution inside the plasma is almost perfectly homogeneous and the discharge behaves like an ideal ion-optical lens. The discharge channels follow very sensitively the laser beams. This can be observed with a very high precision on the scintillator images of the pepperpot beamlets, which oscillate around the discharge axis.

Different targets were tested in the intersection point. It was demonstrated that a current carrying target can be used to guide the discharge current around a fusion pellet, to prevent preheating by the discharge. The target does not disturb the discharge stability and does improve the creation of multiple channels.

For an application of plasma channels in a heavy-ion fusion reactor a discharge current in the order of 50 kA is sufficient.[5] The parameters of the experiment, such as discharge current, channel diameter and stability, and ion optical properties, are therefore very close to the requirements for a fusion reactor. The compatibility of the discharge gas with the fusion chamber environment must be addressed in more detail. The characterization of the discharges by advanced plasma diagnostics and hydro-code simulations will be addressed in a following article.

## ACKNOWLEDGMENT

This work is supported by the German Ministry for Research and Education (BMBF).

[1] A. Tauschwitz *et al.*, Fusion Eng. Des. **32**, 493 (1996).
[2] P. F. Ottinger, D. V. Rose, and D. Mosher, J. Appl. Phys. **70**, 5292 (1991).
[3] J. M. Neri, P. F. Ottinger, D. V. Rose, P. J. Goodrich, D. D. Hinshelwood, D. Mosher, S. J. Stephanakis, and F. C. Young, Phys. Fluids B **5**, 176 (1993).
[4] C. L. Olson, Nucl. Instrum. Methods Phys. Res. A **464**, 118 (2001).
[5] S. S. Yu *et al.*, Nucl. Instrum. Methods Phys. Res. A **415**, 174 (1998).
[6] D. W. Koopman, J. Phys. Colloq. **7**, 419 (1979).
[7] T. Ozaki, A. Yoshinouchi, S. Miyamot, K. Imasaki, S. Nakai, and C. Yamanaka, *Proceedings of the 5th International Conference on High Power Particle Beams*, San Francisco (University of California Press, Berkeley, 1983), pp. 78–81.
[8] T. Ozaki, S. Miyamoto, K. Imasaki, S. Nakai, and C. Yamanaka, J. Appl. Phys. **58**, 2145 (1985).
[9] M. C. Vella, T. J. Fessenden, W. Leemans, S. Yu, and A. Tauschwitz, Nucl. Instrum. Methods Phys. Res. A **415**, 193 (1998).
[10] T. J. Fessenden and M. C. Vella, Plasma Pinch for Transport of HIF Beams, Proceedings of LBNL Conference, Berkeley, California, June 6, 1997.
[11] M. C. Vella, T. J. Fessenden, W. Leemans, and S. Yu, Plasma Pinch for Final Focus and Transport, Proceedings of LBNL-40435 Conference, Berkeley, California, 1996.
[12] C. Niemann, A. Tauschwitz, D. Penache, S. Neff, R. Knobloch, R. Birkner, R. Presura, D. H. H. Hoffmann, S. S. Yu, and W. M. Sharp, J. Appl. Phys. **91**, 617 (2002).
[13] J. N. Olsen, J. Appl. Phys. **52**, 3279 (1981).
[14] J. N. Olsen and L. Baker, J. Appl. Phys. **52**, 3286 (1981).
[15] J. N. Olsen and R. J. Leeper, J. Appl. Phys. **53**, 3397 (1982).
[16] A. Tauschwitz, C. Niemann, D. Penache, R. Birkner, D. H. H. Hoffmann, R. Knobloch, S. Neff, R. Presura, D. Ponce, F. Rosmej, and S. Yu, *Plasma Channel Transport for Heavy Ion Fusion: Investigation of Beam Transport, Channel Initiation and Stability*, AIP Conf. Proc. **650**, 391 (2002).
[17] H. D. Betz, *Applied Atomic Collision Physics*, edited by H. S. W. Massey *et al.*, Pure and Applied Physics, Vol. 43-4 (Academic, Orlando, 1983), p. 1.
[18] S. Yu (private communication, Berkeley, 1996).